ELSEVIER

Biochimica et Biophysica Acta 1190 (1994) 1–8

BBA Biochimica et Biophysica Acta

Time-resolved polarized fluorescence studies of the temperature adaptation in *Bacillus subtilis* using DPH and TMA-DPH fluorescent probes

Petr Heřman [a,*], Ivo Konopásek [b], Jaromír Plášek [a], Jaroslava Svobodová [b]

[a] *Department of Biophysics, Institute of Physics, Charles University, Ke Karlovu 5, 121 16 Prague 2, Czech Republic*
[b] *Department of Microbiology, Faculty of Science, Charles University, Viničná 5, 128 44 Prague 2, Czech Republic*

(Received 8 March 1993)
(Revised manuscript received 20 August 1993)

Abstract

The validity of the concept of homeoviscous adaptation was tested for bacteria *Bacillus subtilis*. The *Bacillus subtilis* grown at 20°C (referred to as Bs20) exhibit a considerable increase of branched anteiso-C_{15}, the major fatty acid component of membrane lipids, relative to membranes grown at 40°C (Bs40). The time-resolved fluorescence depolarization of 1,6-diphenyl-1,3,5-hexatriene (DPH) and 1-[4-(trimethylamino)phenyl]-6-phenyl-1,3,5-hexatriene (TMA-DPH) showed that these changes in the lipid composition are accompanied by changes in a mean lipid order. In particular, the DPH order parameters $\langle P_2 \rangle$ and $\langle P_4 \rangle$ measured in Bs20 membranes at 18°C and in Bs40 membranes at 45°C, respectively, tend to be equal. This effect was less pronounced for TMA-DPH. Our observations suggest that a physical parallel to the changes of lipid composition is the maintenance of an optimal lipid order in the hydrophobic core of the cytoplasmic membranes. It can be interpreted as a tendency of *Bacillus subtilis* to keep the lateral pressure in its membranes at an optimal value, independent of the temperature of cultivation.

Key words: Anisotropy; Membrane; Lipid; Order parameter

1. Introduction

The bacteria serve as a suitable model for examining the temperature adaptation of biological membranes in vivo due to a high metabolic rate and a flexibility of their metabolic regulation. As poikilotherms they reflect the changes in the ambient temperature by adapting the composition of their cytoplasmic membranes [1]. The proportion of unsaturated or branched fatty acids in membrane lipids is increased in response to a lower growth temperature. The theory of 'homeoviscous adaptation' [2] suggests that the 'fluidity' of the lipid bilayer is maintained constant this way, thus enabling vital functions to continue at an optimal condition within a wide range of cultivation temperatures. However, further studies did not validate this concept for all microorganisms [3]. Cossins et al. [4] introduced the quantitative measure of a thermoadaptation called 'homeoviscous efficacy'. It is the extent to which temperature-induced changes of membrane fluidity are compensated by an adjustment of membrane lipid composition. The homeoviscous efficacy equal to one means an adaptation resulting in identical fluidity at different cultivation temperatures. The homeoviscous efficacy of different procaryotic membranes varies from 0.1 to 1 [4] and depends not only on the physiology of given species, but also on the technique and/or probe used [5].

The homeoviscous adaptation of *Bacillus subtilis* was previously tested using steady-state fluorescence anisotropy of 1,6-diphenyl-1,3,5-hexatriene (DPH) in intact cells, isolated membranes and vesicles made of isolated phospholipids. EPR experiments with a spin probe 16-doxylstearate in isolated membranes and phospholipid vesicles were also performed [6–8]. The analysis of fatty acid composition and phospholipid classes revealed a significant difference between cells

* Corresponding author. Fax: +42 2 296764.

SSDI 0005-2736(93)E0286-J

cultivated at 20°C and 40°C (Bs20 and Bs40, respectively). The content of a major fatty acid component, branched anteiso-15, increases from 39% in Bs40 membranes to 55% in Bs20. Suutari et al. [9] have recently measured qualitatively the same dependence of the membrane composition on cultivation temperature. A considerably lower DPH fluorescence anisotropy was found in Bs40 membranes at 40°C relative to Bs20 membranes at 20°C despite changes in the lipid composition. The corresponding homeoviscous efficacy was approximately 0.1. Similar results were obtained with the 16-doxylstearate spin probe. Such data suggested that the temperature-induced adjustment of lipid composition is reflected only in minor changes in *Bacillus subtilis* cell membrane fluidity.

The aim of the present work was to extend the previous study by using time-resolved fluorescence depolarization of DPH and 1-[4-(trimethylamino)phenyl]-6-phenyl-1,3,5-hexatriene (TMA-DPH). In contrast to steady-state fluorescence techniques, this experimental approach can distinguish between simultaneous changes of a probe's lifetimes, its equilibrium angular distribution inside a membrane and rotational diffusion. It offers a deeper insight into the origin of fluorescence signal changes accompanying thermoadaptation and helps to identify which physical properties of the membrane are adjusted by thermoadaptation (for review see e.g. Ref. 10).

2. Materials and methods

2.1. Cultivation of bacteria

Bacillus subtilis 168 trp2-cells were grown aerobically in a complex medium containing (in g/l): Bacto beef extract (Difco) 1.5, Yeast extract (Difco) 1.5, NaCl 3.5, KH_2PO_4 1.32, Bacto peptone (Difco) 5, glucose 5 (pH 7.0). The cultivation was terminated in the mid-exponential phase and cells were harvested by rapid filtration through a Millipore filter (pore size 0.6 μm).

2.2. Membrane preparation

The isolation procedure was similar to that of Bohin et al. [11], except that the temperature was kept identical with the temperature of cultivation in all isolation steps.

The cells remaining on the filter were washed in phosphate buffer (100 mM, pH 7.3) and resuspended in the same buffer containing sucrose (0.5 M). The membrane suspension (about 12 μg wet mass per ml) was incubated (without mixing) with lysozyme (500 μg/ml). The formation of protoplasts was completed within 20 min at 40°C or 50 min at 20°C. The protoplasts were centrifuged for 30 min at 9000 $\times g$ and the pellet was rehomogenized in phosphate buffer (pH 7.3) at a concentration of 1 g wet mass per ml.

RNAase and DNAase were then added (both 0.5 mg per g of wet mass) together with $MgSO_4$ (10 mmol/l). Cell lysis was carried out by a 100-fold dilution of this mixture into a hypotonic phosphate buffer (50 mM, pH 6.6). After 15 min (30 min) of mixing at 40°C (20°C), EDTA (10 mmol/l) was added and another portion of $MgSO_4$ (10 mmol/l) was added 45 min (60 min) later. The cell lysate was centrifuged for 90 min at 30000 $\times g$ and the membrane pellet was washed in a phosphate buffer (50 mM, pH 6.6) containing KCl (1 M) and EDTA (10 mM). The last step was performed for both Bs40 and Bs20 membranes at 0°C. The sediment was rehomogenized in the phosphate buffer (50 mM) with KCl (1 M) at a concentration range of 15–20 mg of membrane protein per ml. Protein concentration was determined according to the Lowry method [12]. Samples were stored at −60°C.

Membrane preparations (only thawed once) were used for fluorescence measurements.

2.3. Cell membrane labelling

Membrane suspensions were diluted in phosphate buffer (100 mM, pH 7.0) to the concentration of 60–100 μg/ml of membrane protein. A DPH solution (3 mM) in acetone or a TMA-DPH solution (0.5 mM) in ethanol was diluted (1 : 1000 v/v) in a vigorously stirred membrane suspension. The labelled suspension was incubated for 30 min at 25°C.

2.4. Pulse-excitation fluorescence measurements

An apparatus for time-resolved fluorescence experiments was based on a laser excitation source and a time-correlated single photon counting detection system. The excitation source was comprised of a cavity dumped dye laser synchronously pumped by an actively mode-locked argon ion laser and frequency doubler. The excitation pulses with a repetition rate of 4 MHz and duration of 10–15 ps were generated at 365 nm with Pyridine 1 as a laser dye. The emission wavelength (425 nm) was selected by a monochromator. Three polarized fluorescence decay curves $I_{\parallel}$, $I_{\perp}$ and I_m were measured with the emission polarizer oriented parallely, perpendicularly and at the angle of 54.7° to the direction of excitation polarization vector, respectively. All three components were accumulated quasi-simultaneously with a switching frequency of 6 s. The apparatus response function was determined from the time profile of the Raman scattering of concentrated aqueous solution of KI at 417 nm. Samples, placed in thermostated holder, were periodically mixed by nitrogen bubbles. All experiments were immediately repeated with an aliquot of an unlabeled sample in order

to accumulate correction curves containing background fluorescence and light scattering. These correction curves were subtracted before deconvolution analysis from the decays of the labeled sample. The correction, main contribution of which was fluorescence of buffer, never exceeded 2% of the total intensity.

2.5. Time-resolved fluorescence data processing

The global data analysis was based on a solution of a convolution integral:

$$I(t) = \int_0^t R(t')i(t-t')\,dt' \quad (1)$$

where $I(t)$, $R(t)$ and $i(t)$ are the observed fluorescent decay, an apparatus response function and a fluorescent decay for an infinitely short excitation pulse, respectively. For the estimation of the impulse response $i(t)$ the Marquardt-Levenberg least squares fitting procedure was used. In order to enhance the significance of the fitted parameters, three different polarization components $i_{\parallel}(t)$, $i_{\perp}(t)$ and $i_m(t)$ were simultaneously fitted (see e.g., Ref. 13) to the corresponding experimental data sets:

$$i_{\parallel} = \tfrac{1}{3}\left[A_1 e^{-t/\tau_1} + A_2 e^{-t/\tau_2}\right] \cdot [1 + 2r(t)] \quad (2a)$$

$$i_{\perp} = \tfrac{1}{3}\left[A_1 e^{-t/\tau_1} + A_2 e^{-t/\tau_2}\right] \cdot [1 - r(t)] \quad (2b)$$

$$i_m = \left[A_1 e^{-t/\tau_1} + A_2 e^{-t/\tau_2}\right] \quad (2c)$$

Under the 'magic angle' condition the measured intensity I_m equals a total component, $I_{\parallel} + 2I_{\perp}$, irrespective of a rotational diffusion of a chromophore. Thus it provides unbiased information about excited state lifetimes. The time-resolved anisotropy, $r(t)$, was fitted to the 'general model' of DPH and TMA-DPH fluorescence depolarization in membranes as previously described [14]. Using this approach, $r(t)$ is a function of four parameters: a zero-time anisotropy r_0, a rotational diffusion coefficient of the long axis of the probe, $D_{\perp}$, and order parameters $\langle P_2 \rangle$ and $\langle P_4 \rangle$. The order parameters are related to the equilibrium angular distribution function $P_{eq}(\theta)$ of the probe molecule and characterize the order of membrane lipid chains. The $\langle P_2 \rangle$ and $\langle P_4 \rangle$ can be expressed as:

$$\langle P_2 \rangle = \int P_{22}(\cos\theta) P_{eq}(\theta) \sin\theta\, d\theta \quad (3a)$$

$$\langle P_4 \rangle = \int P_{24}(\cos\theta) P_{eq}(\theta) \sin\theta\, d\theta \quad (3b)$$

where $P_{22}(\theta)$ and $P_{24}(\theta)$ are Legendre polynomials. For the full characterization of $P_{eq}(\theta)$ it is necessary to have all order parameters $\langle P_{2k} \rangle$ ($k = 1, 2, .., \infty$). Having only $\langle P_2 \rangle$ and $\langle P_4 \rangle$, the distribution $P_{eq}(\theta)$ may be approximated by the 'broadest possible' distribution which is consistent with these $\langle P_2 \rangle$ and $\langle P_4 \rangle$. According to the information theory [15] the $P_{eq}(\theta)$ is given by:

$$P_{eq}(\theta) \sim \exp\left[\lambda_2 P_{22}(\theta) + \lambda_4 P_{24}(\theta)\right] \quad (4)$$

where parameters λ_2 and λ_4 are calculated from Eqs. (3) and (4).

2.6. Steady-state anisotropy measurements

Steady-state anisotropy was measured using a SLM 4800S fluorometer equipped with a standard polarization accessory. The excitation wavelength was 360 nm and emission was detected through cut-off filters, 50% transmittance at 405 nm, in both emission channels. The sample temperature was kept constant with a precision of 0.2 C°. The steady-state anisotropy was calculated as previously described [16].

The experimental data were corrected for an intrinsic fluorescence of unlabeled membranes which never exceeded 1% of the labeled samples. Despite the low background signal several experiments were repeated at a different concentration of membranes. No significant changes in steady-state anisotropy value were detected.

3. Results

3.1. Fluorescence lifetime measurements

The fluorescent intensity decays of both DPH and TMA-DPH can be satisfactorily recovered in terms of a double-exponential decay model, $I(t) = A_1 \exp(-t/\tau_1) + A_2 \exp(-t/\tau_2)$. Improvement of the fit was negligibly small with a triple-exponential model relative to the biexponential one. Moreover, two of the lifetimes assessed from the triple-exponential model were equal to those obtained from the biexponential fitting and fractional amplitudes of the third component, A_3, were always lower than 0.01.

Biexponential decays of DPH fluorescence comprise a component with a lifetime of $\tau_2 = 6$–9 ns (Figs. 1 and 2), which is close to the DPH fluorescence lifetimes in pure organic solvents [17] (for review see also Ref. 18). The lifetimes of the faster decaying component, τ_1, were within the range of 1–2 ns. The fractional amplitudes of this decay component are depicted in Fig. 3.

The τ_2 lifetimes of DPH, as well as the related fractional amplitudes are sensitive to the cultivation temperature of bacteria. The Bs20 membranes exhibited τ_2 lifetimes that were significantly lower than those of Bs40 membranes, Fig. 1. The fractional amplitudes, A_2, of this longer component were also smaller in Bs20 membranes. In contrast to τ_2, there was no significant difference between τ_1 values of Bs20 and Bs40 samples. An increase in temperature decreases τ_2

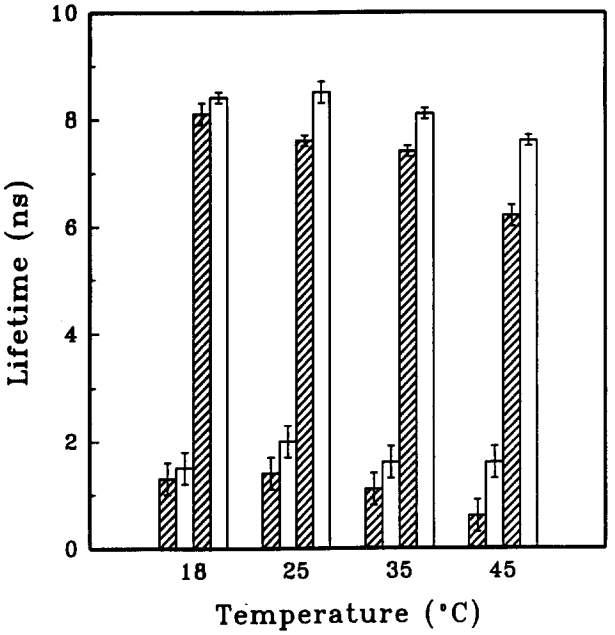

Fig. 1. Fluorescent lifetimes of DPH in cytoplasmic membranes of *Bacillus subtilis*; membranes Bs20 (shaded bars), membranes Bs40 (open bars), τ_1 (short bars), τ_2 (long bars).

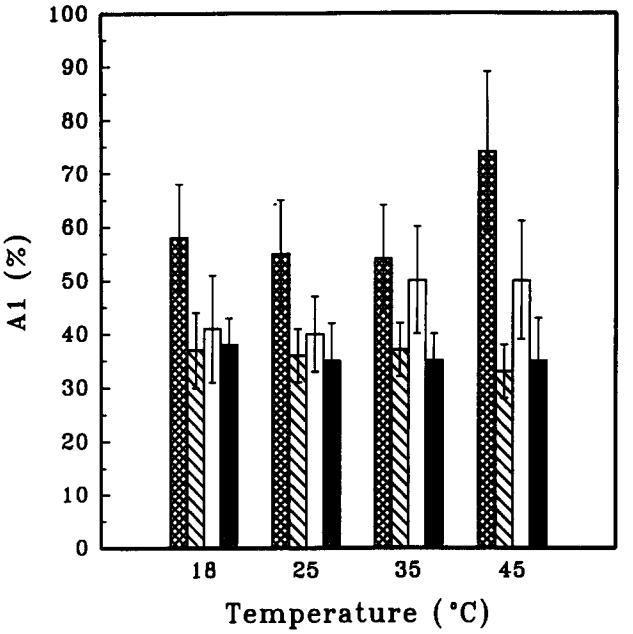

Fig. 3. Amplitudes A_1 of the shorter fluorescent component τ_1; DPH in Bs20 membranes (cross-hatched bars), DPH in Bs40 membranes (coarse hatched bars), TMA-DPH in Bs20 membranes (open bars), TMA-DPH in Bs40 membranes (fine hatched bars).

while changes of τ_1 do not exceed a limit of an experimental error. The temperature-dependent changes of τ_2 are more pronounced in Bs20 membranes relative to those of the Bs40 (Fig. 1).

TMA-DPH fluorescence decay characteristics differ from the results of DPH assays (Fig. 2). The main differences can be summarized as follows:

(i) the temperature-dependent decrease of the TMA-DPH lifetime τ_2 is faster,

(ii) the fractional amplitudes of the faster decaying component are lower than those of DPH fluorescence (Fig. 3) and

(iii) TMA-DPH fluorescence decay parameters do not indicate any remarkable differences between Bs20 and Bs40 membranes.

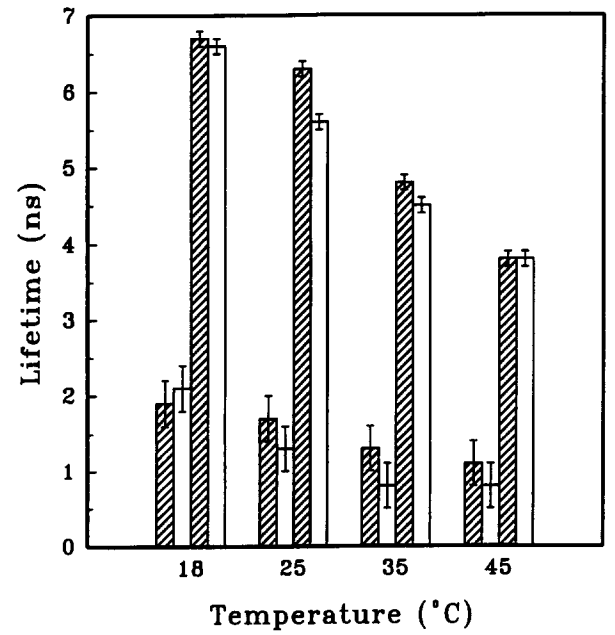

Fig. 2. Fluorescent lifetimes of TMA-DPH in cytoplasmic membranes of *Bacillus subtilis*; membranes Bs20 (shaded bars), membranes Bs40 (open bars), τ_1 (short bars), τ_2 (long bars).

3.2. Steady-state fluorescence anisotropy measurements

Steady-state fluorescence anisotropies, r_{ss}, were measured in the temperature interval from 5°C to 60°C. A gradual decrease of r_{ss} was observed with increasing temperature. This trend was more pronounced in DPH-labeled membranes (Fig. 4). For both probes the r_{ss} value was significantly lower in Bs20 membranes compared to the Bs40 ones. The difference in r_{ss}, between Bs20 and Bs40 membranes, was larger in the case of DPH which is similar to the analysis of lifetimes.

3.3. Time-resolved fluorescence depolarization experiments

The analysis of time-resolved fluorescence anisotropy was carried out by two different methods. In the first method the zero-time anisotropy r_0 was fixed to the value of 0.38 (the fluorescence anisotropy of

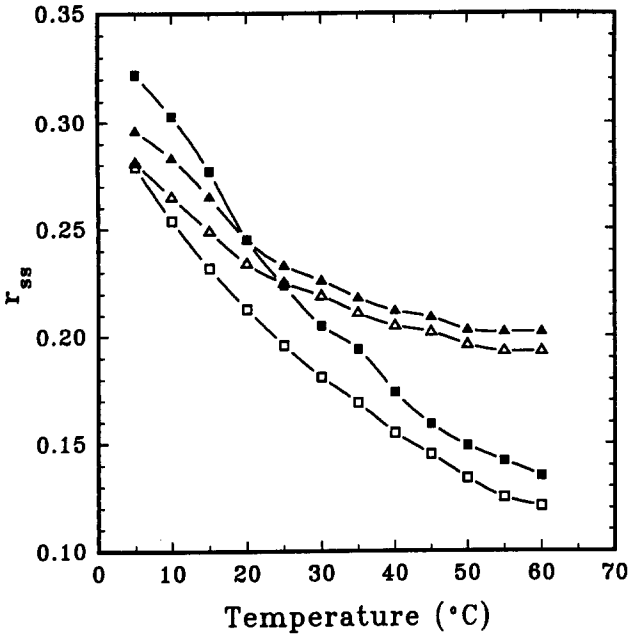

Fig. 4. Steady-state fluorescence anisotropy of DPH (■) and TMA-DPH (▲) in the *Bacillus subtilis* Bs20 (open symbols) and Bs40 (closed symbols) cytoplasmic membranes.

DPH immobilized in frozen glycerol [19]) but in the second method the r_0 was optimized as a floating parameter. Results of the latter approach were found to be more satisfying. The first approach resulted in an unacceptably poor fit in some cases.

The fitted values of r_0 are shown in Table 1. They fall within the range of zero-time anisotropies reported

Table 1
Zero-time anisotropies r_0 of DPH and TMA-DPH in *Bacillus subtilis* cytoplasmic membranes

Probe/Sample	Sample temperature/limiting anisotropy r_0			
	18°C	25°C	35°C	45°C
DPH/Bs20	0.36 (0.02)	0.35 (0.01)	0.37 (0.01)	0.33 (0.02)
DPH/Bs40	0.38 (0.01)	0.37 (0.01)	0.34 (0.02)	0.33 (0.02)
TMA-DPH/Bs20	0.40 (0.02)	0.36 (0.01)	0.36 (0.01)	0.37 (0.01)
TMA-DPH/Bs40	0.38 (0.01)	0.40 (0.02)	0.38 (0.01)	0.38 (0.01)

Numbers in parentheses represent standard deviations of r_0 fitted as a floating parameter.

for the DPH and TMA-DPH fluorescence in a variety of frozen solutions (see e.g., Ref. 19 for review) and tend to decrease with increasing temperature. This tendency was found to be significant for DPH in Bs40 membranes.

Fitted order parameters and their standard deviations are shown in Fig. 5A (DPH) and Fig. 5B (TMA-DPH). Corresponding distribution functions $P_{eq}(\theta)$ were also calculated (Eqs. (3) and (4)). However, estimations of $P_{eq}(\theta)$, based on $\langle P_2 \rangle$ and $\langle P_4 \rangle$ only, was found to be incredibly sensitive to an experimental error of $\langle P_4 \rangle$. Fig. 6 shows the difference between distribution functions calculated for one of the experimental conditions using the same $\langle P_2 \rangle$ and three different $\langle P_4 \rangle$ values, which were chosen from the interval of $\langle P_4 \rangle$ experimental error. Changes in the shape of $P_{eq}(\theta)$ were so large that such a representation loses informational value. We have therefore preferred the

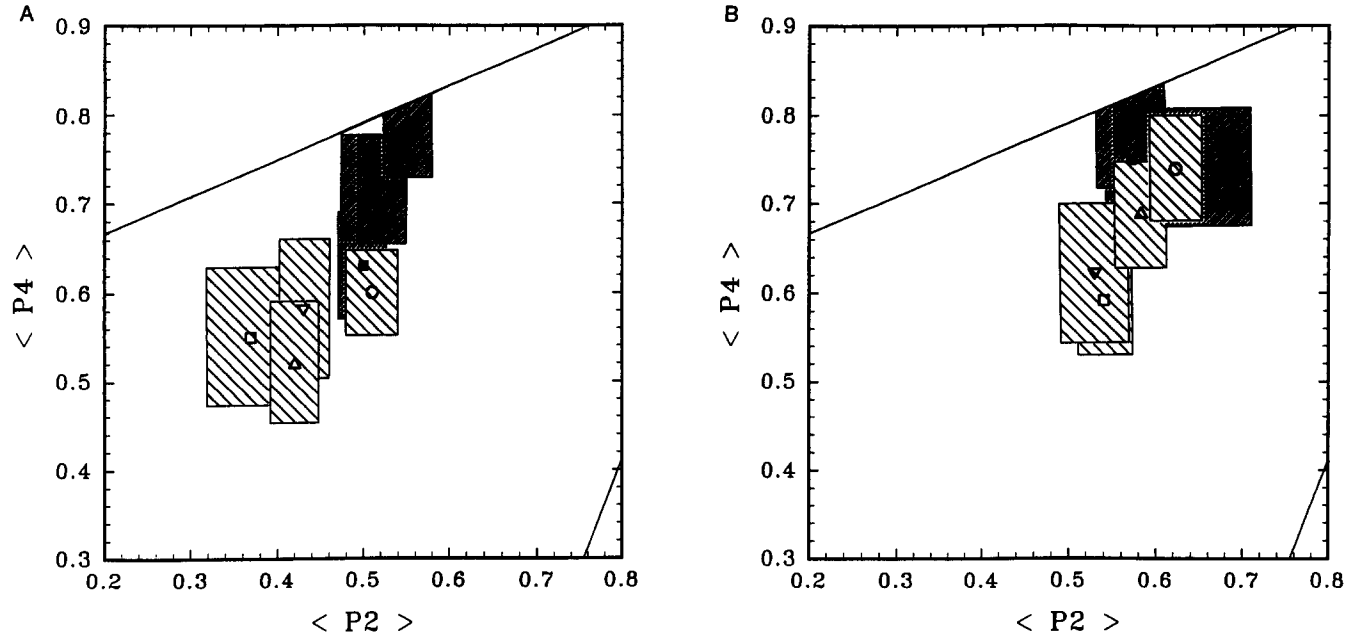

Fig. 5. Order parameters $\langle P_2 \rangle$ and $\langle P_4 \rangle$ of DPH (A) and TMA-DPH (B) in the cytoplasmic membranes of *Bacillus subtilis* at different temperatures; (●) 18°C, (▼) 25°C, (▲) 35°C, (■) 45°C. Open and closed symbols denote the order parameters for membranes Bs20 and Bs40, respectively. Rectangles represent the most probable locations of the respective points and are defined by standard deviations of the order parameters. The solid lines border the region of allowed values of the $\langle P_2 \rangle$ and $\langle P_4 \rangle$.

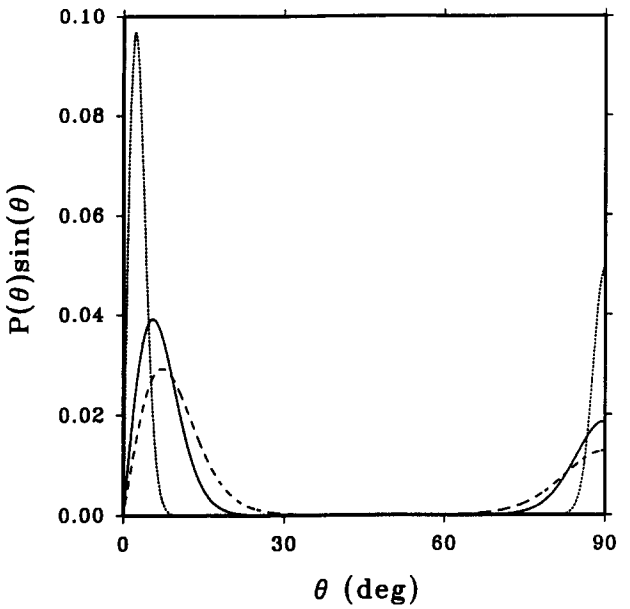

Fig. 6. An equilibrium angular distribution of TMA-DPH in Bs40 membranes at 45°C and its dependence on the error of the $\langle P_4 \rangle$ assessment. Distribution functions were calculated for $\langle P_2 \rangle = 0.57$ and mean value $\langle P_4 \rangle = 0.75$ (solid line), upper confidence limit $\langle P_4 \rangle = 0.81$ (dotted line), lower confidence limit $\langle P_4 \rangle = 0.69$ (dashed line).

position of a $[\langle P_2 \rangle, \langle P_4 \rangle]$ point in the $\langle P_2 \rangle$ vs. $\langle P_4 \rangle$ diagram as more reliable characteristics of the probe angular equilibrium distribution in membranes.

The information derived from the $\langle P_2 \rangle$ vs. $\langle P_4 \rangle$ diagrams is summarized below:

(i) $\langle P_2 \rangle$ order parameters of DPH are lower than those of TMA-DPH in both Bs20 and Bs40 membranes. The comparison is made for the same membrane system at the same temperature.

(ii) Both $\langle P_2 \rangle$ and $\langle P_4 \rangle$ order parameters of DPH tend to decrease with increasing temperature. A magnitude of the change of $\langle P_2 \rangle$ seems to be smaller in Bs40 membranes than that in Bs20 membranes (Fig. 5A). Such effects were not found for TMA-DPH (Fig. 5B).

(iii) Both $\langle P_2 \rangle$ and $\langle P_4 \rangle$ order parameters for DPH are systematically lower in Bs20 than in Bs40 membranes when the different membranes are compared at the same temperature. A similar systematic difference was observed for TMA-DPH, but it was found to be less significant. In particular, $\langle P_2 \rangle$ order parameters of TMA-DPH in both types of membranes are very similar.

(iv) The order of Bs20 and Bs40 membranes, respectively, probed by DPH and characterized by a localization of the $[\langle P_2 \rangle, \langle P_4 \rangle]$ point in the $\langle P_2 \rangle$ vs. $\langle P_4 \rangle$ diagram (Fig. 5A), exhibit a tendency to coincide when the experimental temperature approaches the temperature of cultivation. This is indicated by an overlap of the confidence areas demarcated by the confidence intervals of the each point. Particularly, the order parameters $\langle P_2 \rangle$ and $\langle P_4 \rangle$ within an experimental error are the same for Bs20 at 18°C and Bs40 at 45°C. The difference in the membrane order becomes significant when different membranes are compared at the same temperature. Such a behavior seems to be the most interesting feature of the temperature-dependent changes of the order parameters.

This effect is less remarkable for TMA-DPH. The larger deviation of experimental temperature from the temperature of cultivation results in approximately the same order of Bs20 and Bs40 membranes, respectively. (See the overlap of confidence areas between Bs20 and Bs40 membranes, respectively; Fig. 5B.)

Values of the rotational diffusion coefficient $D_\perp$, of both DPH and TMA-DPH ranged from $2.6 \cdot 10^8$ to $2.0 \cdot 10^9$ s^{-1}. The confidence intervals of $D_\perp$ was found to be the largest of the all fitted parameters. Relative errors ranged from −70 to +300%. Therefore the observed changes of $D_\perp$ are not significant within this experimental error.

4. Discussion

4.1. Fluorescence lifetime measurements

The biexponential decay of DPH fluorescence observed in membranes of *Bacillus subtilis* is in accord with typical characteristics of DPH fluorescence in other membrane systems. The fact that in Bs20 membranes the τ_2 lifetimes of DPH are lower than those in Bs40 ones, Fig. 1, suggests that there exists a difference in physical properties of the respective probe microenvironments. It was demonstrated earlier that the DPH fluorescent lifetimes in synthetic lipid vesicles tend to decrease with increasing lipid unsaturation [20]. We therefore conclude that the observed difference between lifetimes in Bs20 and Bs40 membranes is consistent with known variations of branched and unsaturated fatty acids in the phospholipids of these membranes [6].

Apparent lifetimes of TMA-DPH fluorescence in *Bacillus subtilis* membranes are basically independent of variations in the lipid composition. The different behavior of DPH and TMA-DPH could be explained by their different localization in membranes. The TMA-DPH, which is anchored by the trimethylammonium moiety to the polar head region, selectively probes a membrane structure near the membrane surface while the DPH mainly probes a lipid structure inside the membrane core. Therefore the similarity of TMA-DPH lifetimes in Bs20 and Bs40 membranes indicates that the thermoadaptive control of the lipid composition is

not accompanied by significant changes in physical properties of the probe microenvironment near the polar head region.

4.2. Steady-state anisotropy

The steady-state anisotropy experiments indicate that *Bacillus subtilis* has a tendency to fluidize its cytoplasmic membrane during the process of thermoadaptation, as was already demonstrated for DPH [6]. The difference in respective r_{ss} values of Bs20 membranes at 20°C and Bs40 membranes at 40°C (Fig. 4) is consistent with the fact that both the steady-state anisotropy of DPH fluorescence and spin probe spectra do not reveal a complete homeoviscous adaptation. However, our present analysis of fluorescent decays in these systems suggests that the results of the steady-state DPH fluorescence depolarization assays could be significantly affected by parallel variations in DPH fluorescent lifetimes. Thus the simple technique of steady-state fluorescence depolarization becomes unsuitable for a reliable examination of physical aspects of the lipid control during thermoadaptation.

Similarly, no explicit conclusions on the physical properties of lipid membranes can be easily made from single changes of line intensities in EPR probe spectra mentioned above [6]. An interpretation of a spin probe spectra requires complex simulations including order parameters and correlation times for rotation around the main molecular axis and for rotation of that axis [21]. This technique, however, has not been elaborated yet to an extent comparable with the method of time-resolved fluorescence depolarization. Currently, the latter approach can provide the most explicit information about rotational diffusion of the probe and its angular equilibrium distribution inside the membrane.

4.3. Time-resolved fluorescence depolarization

The difference between order parameters in Bs20 and Bs40 membranes reveals that the thermoadaptive changes of their lipid composition are accompanied by changes in a lipid order. In particular, it can be concluded that the modification of lipid composition at the low cultivation temperature induces a decrease in the membrane lipid order. Moreover, the DPH order parameters determined in Bs20 membranes at 18°C and Bs40 membranes at 45°C tend to be equal, Fig. 5A. This fact suggests that the physical parallel to the thermoadaptive changes of the membrane lipid composition is the maintenance of an optimal lipid order. The lower sensitivity of TMA-DPH order parameters to the thermoadaptation indicates that the latter conclusion is valid particularly for the core of the membrane. Lower order parameters for DPH, compared to TMA-DPH, reveal the well-known existence of the lipid order gradient between the membrane core and its surface [22,23].

Our analysis of DPH and TMA-DPH order parameters in *Bacillus subtilis* membranes seems to support an idea that a possible function of the thermoadaptive exchange of membrane lipids is to preserve an optimal order of the lipid bilayer. It has been demonstrated earlier that the lipid order can be directly related to a lateral pressure which is experienced by other membrane components [24]. The lateral pressure, which increases with decreasing lipid order, can modulate an activity of certain membrane enzymes [25,26]. From this point of view the changes of the lipid order of *Bacillus subtilis*, mediated by changes in membrane lipid composition, could be eventually interpreted as a tendency for maintaining an optimal value of the lateral pressure in plasma membranes.

5. Acknowledgements

We thank Dr. Erica Pyles for her assistance in the preparation of the manuscript.

6. References

[1] Marr, A.G. and Ingraham, J.L. (1962) J. Bacteriol. 84, 1260–1267.
[2] Sinensky, M. (1974) Proc. Natl. Acad. Sci. USA 71, 522–525.
[3] McElhaney, R.N. (1984) in Membrane fluidity (Kates, M. and Manson, L.A., eds.) pp. 249–278, Plenum Press, New York.
[4] Cossins, A.R. and Sinensky, M. (1984) in Physiology of membrane fluidity, Vol. 2 (Shinitzky, M., ed.), pp. 1–20, CRC Press, Boca Raton, FL.
[5] Rottem, S., Markowitz, O. and Razin, S. (1978) Eur. J. Biochem. 85, 450–455.
[6] Svobodová, J., Julák, J., Pilař, J. and Svoboda, P. (1988) Folia Microbiol. 33, 1170–1177.
[7] Svobodová, J. and Svoboda, P. (1988) Folia Microbiol. 33, 1–9.
[8] Svobodová, J. and Svoboda, P. (1988) Folia Microbiol. 33, 161–169.
[9] Suutari, M. and Laakso, S. (1992) Biochim. Biophys. Acta 1126, 119–124.
[10] Lentz, B.L. (1989) Chem. Phys. Lipids 50, 171–190.
[11] Bohin, J.P., Bohin, A. and Schaeffer, P. (1976) Biochimie 58, 99–108.
[12] Lowry, O.H., Rosebrough, N.J., Farr, A.L. and Randall, R.J. (1951) J. Biol. Chem. 193, 2630–272.
[13] Eisenfeld, J. and Ford, C.C. (1979) Biophys. J. 26, 73–83.
[14] Van der Meer, W., Pottel, H., Herreman, W., Ameloot, M., Hendrickx, H. and Schröder, H. (1984) Biophys. J. 46, 515–523.
[15] Berne, J.B., Pechukas, P. and Harp, G.D. (1968) J. Chem. Phys. 49, 3125–3129.
[16] Lakowicz, J.R. (1983) Principles of fluorescence spectroscopy, Plenum Press, New York, London.
[17] Cehelnik, E.D., Cundall, R.B., Lockwood, J.R. and Palmer, T.F. (1975) J. Phys. Chem. 79, 1369–1376.
[18] Dale, R.E. (1983) in Time-resolved fluorescence spectroscopy in biochemistry and biology (Cundall, R.B. and Dale, R.E., eds.), pp. 555–612, NATO ASI Ser. A69, Plenum Press, New York.

[19] Ameloot, M., Hendrickx, H., Herreman, W., Pottel, H., Van Cauwelaert, F. and Van der Meer, W. (1984) Biophys. J. 46, 525–539.
[20] Stubbs, C.D. and Smith, A.D. (1984) Biochim. Biophys. Acta 779, 89–137.
[21] Schreier, S., Polnaszek, C.F. and Smith, I.C.P. (1978) Biochim. Biophys. Acta 515, 395–436.
[22] Seelig, A. and Seelig, J. (1974) Biochemistry 13, 4839–4845.
[23] Seelig, J. and Waespe-Sersevic, N. (1978) Biochemistry 16, 45–50.
[24] Fulford, A.J.C. and Peel, W.E. (1980) Biochim. Biophys. Acta 598, 237–246.
[25] Owicky, J.C., Springgate, M.W. and McConnel, H.M. (1978) Proc. Natl. Acad. Sci. USA 75, 1616–1619.
[26] Amler, E., Jasinska, R., Drahota, Z. and Zborowski, J. (1990) FEBS Lett. 271, 165–168.